Establishment of Stable Cell Lines—Stable HEK293 cell lines that express miR-143 were generated by selection with 300 μg/ml Geneticin. HEK293 cells were transfected with 0.5 μg of the pri-miR-143 expression vector at 90% confluency in 24-well dishes using a Lipofectamine LTX reagent in accordance with the manufacturer's instructions. Twelve hours after the transfection, the cells were re-plated in a 10-cm dish followed by a 3-week selection with the antibiotic. Ten surviving single colonies were picked up from each transfectant and then cultured for another 2 weeks. The cells expressing the largest amount of miR-143 among transfectants were used as miR-143 stably expressing cells.

Luciferase Reporter Assay—HEK293 cells were cultured at a density of 1×10^4 cells/well in 96-well tissue culture plates overnight, and miRNA transfections or the addition of CM was performed. The cells were harvested, and renilla luciferase activity was measured and normalized by firefly luciferase activity (10). All assays were performed in triplicate and repeated at least three times, and the most representative results are shown.

Cell Growth Assay—PC-3M-luc cells were seeded at a density of 2×10^3 cells/well in a 96-well plate. The following day the cells were transfected with mature miRNAs or incubated with a CM. Twenty-four hours later the culture medium of the transfected cells was switched to medium A, whereas the conditioned medium was not changed. After a 3-day culture, cells were harvested for the measurement of firefly luciferase activity. To know the cellular proliferation by the tetrazolium-based colorimetric MTT assay, 20 μl CM of TetraColor ONE (SEIKAGAKU Corp., Tokyo, Japan) was added to each well after 72 h of culture. After 2–4 h of incubation at 37 °C, the optical density was measured at a wavelength of 450 nm using a microplate reader.

PKH67-labeled Exosome Transfer—Purified exosomes derived from PNT-2 CM were labeled with a PKH67 green fluorescent labeling kit (Sigma). Exosomes were incubated with 2 μM PKH67 for 5 min, washed 4 times using a 100-kDa filter (Microcon YM-100, Millipore) to remove excess dye, and incubated with PC-3M-luc cells at 37 °C.

Co-culture Experiment—In co-culture experiments, 2×10^5 cells/well of PNT-2 cells were plated in 6-well plates. To stain the PNT-2 cells with BODIPY-TR-ceramide (Invitrogen), 5 μM BODIPY-TR-ceramide in a non-serum culture medium was added and incubated with the cells at 37 °C. After 30 min the cells were rinsed several times with a non-serum culture medium and incubated in a fresh medium at 37 °C for an additional 30 min. After the staining of PNT-2 cells by BODIPY-TR-ceramide, labeling of PC-3M-luc cells with PKH67 was performed in accordance with the manufacturer's instructions. After that, labeled PC-3M-luc cells were added and co-cultured with PNT-2 cells for 12 h at 37 °C.

Microarray Analysis—To detect the miRNAs in exosomes and cells derived from PNT-2 and PC-3M-luc cells, 100 ng of total RNA was labeled and hybridized using a human microRNA microarray kit (Agilent Technologies) according to the manufacturer's protocol (Protocol for Use with Agilent MicroRNA Microarrays Version 1.5). Hybridization signals were detected using a DNA microarray scanner (Agilent Technologies), and the scanned images were analyzed using Agilent Feature Extraction software.

Evaluation of Tumor-suppressive miRNA Delivery to Subcutaneously Implanted Prostate Cancer Cell Line in Mice—Animal experiments in this study were performed in compliance with the guidelines of the Institute for Laboratory Animal Research, National Cancer Center Research Institute. Seven-week-old male Balb/c athymic nude mice (CLEA Japan, Shizuoka, Japan) were anesthetized by exposure to 3% isoflurane for injections and *in vivo* imaging. Four days ahead of the first CM injection, the anesthetized animals were subcutaneously injected with 5×10^5 PC-3M-luc cells suspended in 100 μl of sterile Dulbecco's phosphate-buffered saline into each dorsal region. Five hundred μl of CM derived from miR-143-overexpressing HEK293 cells and control cells were daily injected into each tumor from day 0 to 6. For *in vivo* imaging, the mice were administered D-luciferin (150 mg/kg, Promega) by intraperitoneal injection. Ten minutes later, photons from animal whole bodies were counted using the IVIS imaging system (Xenogen) according to the manufacturer's instructions. Data were analyzed using LIVINGIMAGE 2.50 software (Xenogen).

RESULTS

Suppression of Prostate Cancer Cell Proliferation by Conditioned Medium Isolated from Non-cancerous Prostatic Cell—Cell competition is a homeostatic mechanism for the accommodation of an appropriate number of cells in a limited niche or stroma (1). Based on this idea it is possible that the cell competition between normal and abnormal cells frequently occurs in a precancerous state. Of note is that non-cancerous cells suppress cancer cell development by contact-independent interaction (12). For instance, endothelial cells provide the major extracellular heparan sulfate proteoglycan as anti-proliferative signals (12); however, the molecular mechanism by which the other types of cells in a tumor environment associate with cancer cells is not fully understood.

To analyze the mechanism, we treated a hormone-insensitive prostatic carcinoma cell line, PC-3M-luc cells, with a CM from the non-cancerous prostate cell line PNT-2 cells. After a 3-day incubation, the PNT-2 CM inhibited the growth of the PC-3M-luc cells up to ~10% compared with the cell growth treated by fresh culture medium (Fig. 1*A*; compare *lanes 1* and *3*). In contrast, the growth of PC-3M-luc cells incubated in the CM of PC-3M-luc cells themselves showed no inhibitory effect (Fig. 1*A*; compare *lanes 1* and *2*). To determine that the performed treatments did not affect the luciferase activity, we also used the colorimetric MTT assay to measure the cell growth of PC-3M-luc cells. As shown in supplemental Fig. 1*A*, not only luciferase assay but also MTT assay show the inhibition of PC-3M-luc cell proliferation by the addition of PNT-2 cells derived CM, indicating that our treatment did not affect the luciferase activity. These results indicate that the non-cancerous cells may secrete some molecules that can suppress cancer cell proliferation.

In a recent report we showed that miRNAs contained in exosomes are secreted and that their secretion is tightly regulated by neutral sphingomyelinase 2, which is known to hydrolyze sphingomyelins to generate ceramides and trigger the budding

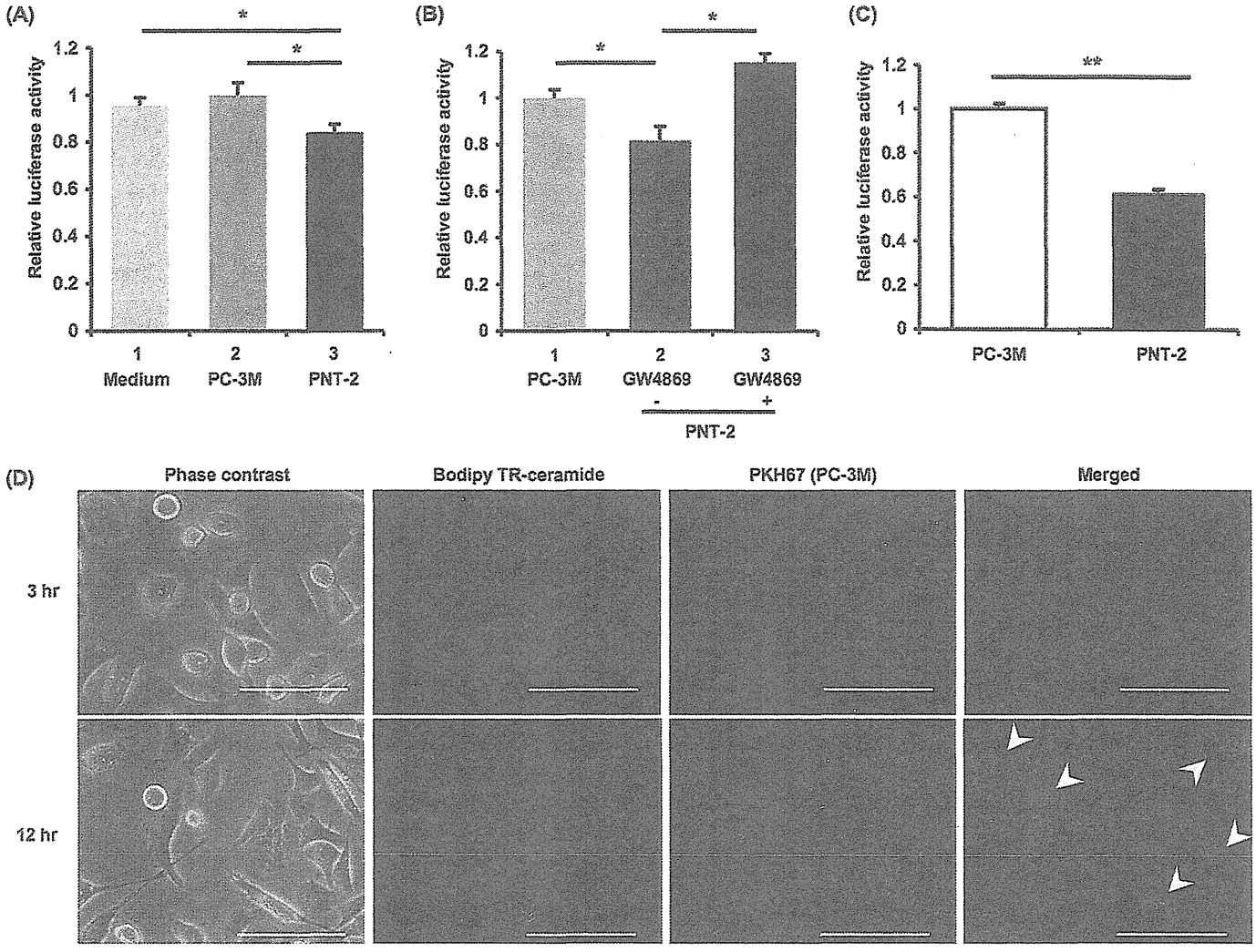

FIGURE 1. **Suppression of cancerous cell proliferation by exosome isolated from non-cancerous cells.** *A*, cell growth inhibition by a conditioned medium derived from PNT-2 cells is shown. PC-3M-luc cells were incubated for 3 days in a conditioned medium isolated from PC-3M-luc cells, PNT-2 cells, or a culture medium followed by a cell growth assay as described under "Experimental Procedures." The values on the *y* axis are depicted relative to the normalized luciferase activity of culture medium-treated cells, which is defined as 1. Each *bar* is presented as the mean S.E. ($n = 3$). *, $p < 0.05$ as compared with culture medium-treated PC-3M-luc cells; Student's *t* test. *B*, treatment with GW4869 to donor cells restored the reduced cell growth by the PNT-2-derived CM is shown. Donor PNT-2 cells were incubated in the presence or absence of 10 μM GW4869 for 2 days. The conditioned medium from PC-3M-luc cells was used as a control. The values on the *y* axis are depicted relative to the normalized luciferase activity of PC-3M-luc-conditioned medium-treated cells, which is defined as 1. Each *bar* is presented as the mean S.E. ($n = 3$). *, $p < 0.05$; Student's *t* test. *C*, cell growth inhibition by exosomes derived from PNT-2 cells is shown. PC-3M-luc cells were incubated in exosomes isolated from PNT-2 cells or PC-3M-luc cells followed by a cell growth assay, as described under "Experimental Procedures." The values on the *y* axis are depicted relative to the normalized luciferase activity of cells treated with exosomes derived from PC-3M-luc cells is defined as 1. Each *bar* is presented as the mean S.E. ($n = 3$). **, $p < 0.005$, as compared with exosomes isolated from PC-3M-luc cells; Student's *t* test. *D*, shown are fluorescent photos of BODIPY-ceramide-labeled PNT-2 and PC-3M-luc cells marked by PKH67. PNT-2 cells and PC-3M-luc cells were labeled with red fluorescent BODIPY-ceramide and green fluorescent PKH67, respectively, as described under "Experimental Procedures." After treatment of PNT-2 by BODIPY-ceramide, PKH67-labeled PC-3M-luc cells were added. After co-culturing for 3 or 12 h, images were obtained. Fluorescent photos were detected with the Eclipse TE 2000 Inverted Research Microscope, and images were produced using NIS-Elements BR software. *Arrowheads* show *yellow colored* cancer cells. The *size bar* indicates 100 μm.

of exosomes. We collected two separate aliquots of CM from PNT-2 cells incubated with or without GW4869, a specific inhibitor for neutral sphingomyelinase 2. The isolated exosomes were verified by the detection of CD63 protein, a well established exosome marker, with immunoblotting (supplemental Fig. 1*B*), and the activity of GW4869 was confirmed by the decreased amount of exosomal protein (supplemental Fig. 1*C*). The CM prepared in the presence of the GW4869 compound cancelled most tumor-suppressive activity of the non-treated PNT-2 CM (Fig. 1*B*; compare *lanes 1–3*). Furthermore, proliferation of PC-3M-luc cells was inhibited by the addition of the exosome fraction isolated from the PNT-2 CM by ultracentrifugation (Fig. 1*C*). These observations suggest that exosomal miRNAs derived from non-cancerous cells were transferred to cancerous cells, resulting in the inhibition of their proliferation.

To visualize the transfer of ceramide-containing exosome from PNT-2 to PC-3M-luc *in vitro*, a co-culture experiment was performed. Before the co-culture, 2×10^5 PNT-2 cells were incubated for 30 min with red fluorescent BODIPY-ceramide dye, which can label the exosomes inside the cells (13, 14). After washing five times with PBS, equal numbers of PC-3M-luc cells labeled by green fluorescent PKH67, a cellular membrane indicator, were added into the culture dishes. Three hours later we did not observe any PC-3M-luc cells with a yellow color (*Merged* photo in *upper panel* of Fig. 1*D*), indicating that car-

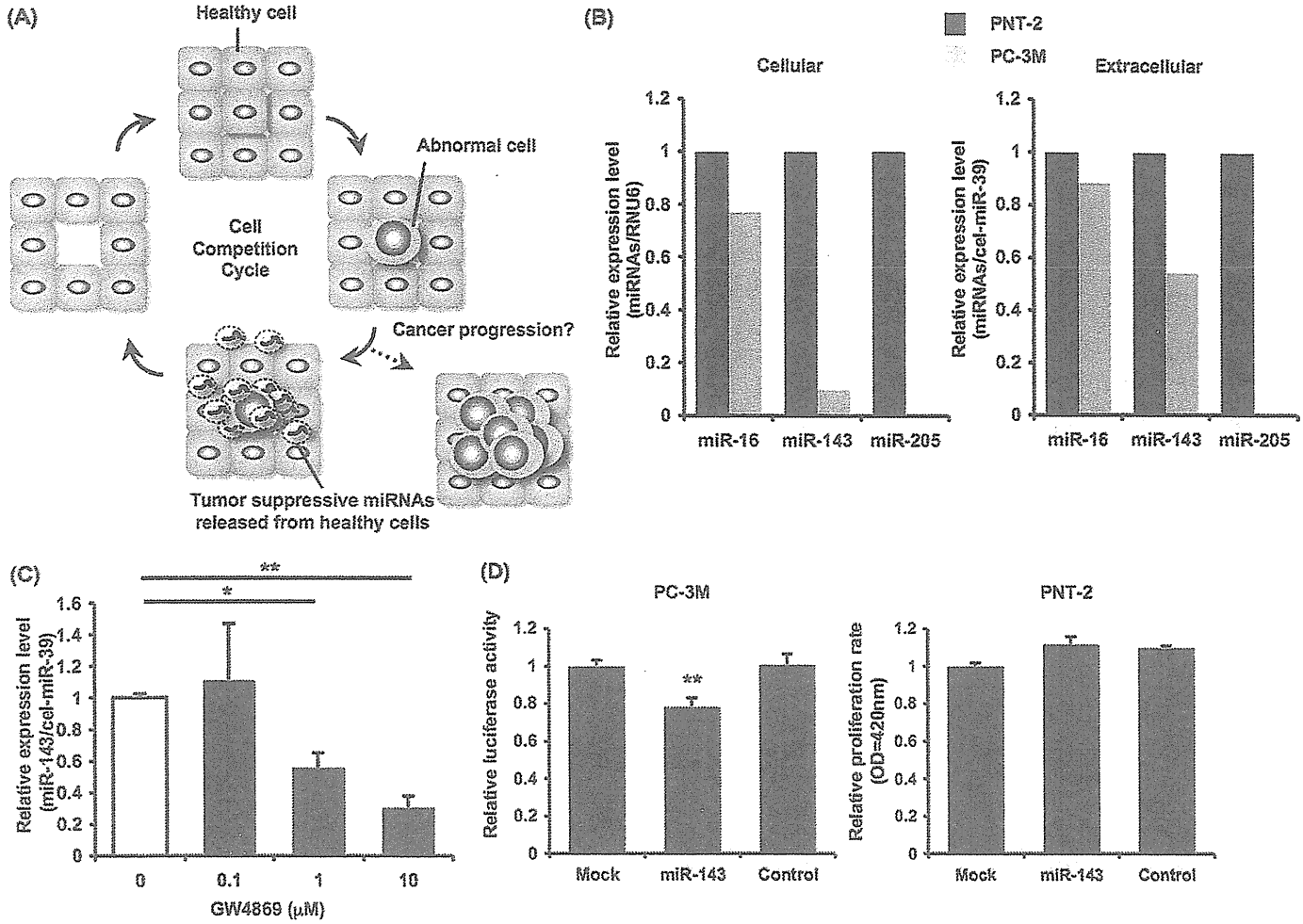

FIGURE 2. **Down-regulation of cellular and extracellular tumor-suppressive miRNAs in PC-3M-luc cells.** *A*, shown is a schematic representation of hypothetical tumor initiation process. Neighboring healthy cells (*blue*) secrete tumor-suppressive miRNAs (*light yellow*) to inhibit the proliferation of abnormal cells (gray), and this cell population returns to the initial healthy condition (a homeostatic cycle). Once the cell competitive cycle is compromised, this niche become susceptible to tumor initiation (indicated by a *dashed arrow*). *B*, comparison of cellular and extracellular miRNAs expression in PNT-2 and PC-3M-luc cells is shown. miRNA expression levels were determined by a Taq-Man QRT-PCR. The values on the *y* axis are depicted relative to the normalized expression level of PNT-2 cells, which is defined as 1. *C*, secretion of miR-143 was suppressed by the treatment with GW4869. PNT-2 cells were seeded and cultured in a 24-well plate for 48 h in the indicated concentrations of GW4869. After the incubation, the medium was subjected to QRT-PCR for miR-143. The values on the *y* axis are depicted relative to the amount of miR-143 at 0 μM GW4869, which is defined as 1. *D*, shown is cell growth inhibition by miR-143 in PC-3M-luc cells but not in PNT-2 cells. PNT-2 and PC-3M-luc cells were transfected with 10 nM miR-143 molecules (miR-143) or 10 nM negative control molecules (control) or without RNA molecules (*Mock*). The values on the *y* axis are depicted relative to the normalized luciferase activity of untreated cells (*Mock*), which is defined as 1. Each *bar* is presented as the mean S.E. ($n = 3$). *, $p < 0.05$; **, $p < 0.005$, as compared with untreated PC-3M-luc cells; Student's *t* test.

ried-over red dyes were thoroughly removed as 3 h is enough time for the dye to be incorporated directly into the cells. By contrast, after 12 h of co-culture, yellow fluorescence was observed in green-labeled PC-3M-luc cells (indicated by *arrowheads* in Merged photo in the *lower panel* of Fig. 1*D*), suggesting that ceramide-containing exosomes from PNT-2 cells were transferred to the PC-3M-luc cells. This result is corroborated by the uptake experiment using the PKH67-labeled exosomes purified from PNT-2 culture medium (supplemental Fig. 1*D*). Green fluorescence was detected in PC-3M-luc cells after 16 h of incubation, providing a direct evidence for exosome uptake by cancerous cells.

Tumor-suppressive miRNAs Down-regulated in Cancerous Cells Were Secreted from Non-cancerous Cells—We propose a hypothetical model of tumor initiation involving cell competition and anti-proliferative secretory miRNAs (Fig. 2*A*). In a cell competition cycle, as illustrated in the *bottom part* of Fig. 2*A*, growth inhibitory miRNAs are actively released from non-cancerous cells to kill abnormal cells with a partial oncogenic ability, thereby restoring them to a healthy state. Indeed, inhibitory capacity of these miRNAs appears to be limited in the setting of single treatment with the PNT-2 CM (Fig. 1*A*); however, they can potentially prevent emergence of tumor cells in a physiological condition. Because abundantly existing healthy cells continuously provide nascent overproliferative cells with tumor-suppressive miRNAs for a long period, a local concentration of secretory miRNAs can become high enough to restrain a tumor initiation. A *dashed arrow* in Fig. 2*A* indicates the way whereby the disruption of the homeostatic system leads to tumor expansion. If precancerous cells acquire resistance to anti-proliferative secretory miRNAs or normal cells cannot supply an adequate amount of miRNAs, then this defensive system will fail to maintain the healthy condition.

To test this hypothesis we checked the secretion amount of representative tumor-suppressive miRNAs by comparing PNT-2 and PC-3M-luc cells with Taq-Man QRT-PCR analysis. As shown in Fig. 2*B*, miR-16, miR-205, and miR-143, which are already reported to be dysregulated in prostate cancer (10, 15, 16), were down-regulated in PC-3M-luc cells at a cellular and extracellular level. The GW4869 inhibitor suppressed the secretion of miR-143 from PNT-2 cells in a dose-dependent manner (Fig. 2*C*), whereas its cellular level was not altered (supplemental Fig. 2*A*). Additionally, the application of small interfering RNAs specific for human neutral sphingomyelinase 2 gene knocked down its mRNAs, resulting in profound decrease in miR-143 secretion (supplemental Fig. 2, *B* and *C*). On the contrary, the expression of miR-143 in the cells was not changed after the transfection of neutral sphingomyelinase 2 siRNA (supplemental Fig. 2*D*). Taken with the result of Fig. 1*B*, these results suggest that the secreted tumor-suppressive miRNAs are implicated in the process of growth inhibition by PNT-2 CM.

For a global understanding of the expression change of non-cancerous and cancerous cells, we performed an miRNA microarray analysis against cellular and exosomal RNAs purified from PNT-2 and PC-3M-luc cells. In the sub-dataset of secretory exosomal miRNAs from PNT-2 cells, we found 40 miRNAs whose cellular amounts were lowered by one-half in PC-3M-luc cells (Table 1). The selected miRNAs expectedly include several types of tumor-suppressive miRNAs, such as miR-15a, miR-200 family, miR-148a, miR-193b, miR-126, and miR-205 (10, 15, 17–20). This observation supports the idea that secretory tumor-suppressive miRNAs are transferred from non-cancerous cells to cancerous cells, in accordance with the concentration gradient of the miRNA.

We have so far demonstrated that normal cells have a higher secretion of tumor-suppressive miRNAs than cancerous cells; however, it remains unclear whether or not these secreted miRNAs affect the proliferation of cells of their origin. To answer this question, we introduced synthesized miR-143 to both PNT-2 and PC-3M-luc cells and assessed their proliferation rates. After 3 days of transfections, the miR-143 analog induced growth inhibition of PC-3M-luc cells compared with mock and control small RNA transfection (Fig. 2*D*, *left panel*). In contrast, the exogenously transduced miR-143 did not show its anti-proliferative effect in PNT-2 cells (Fig. 2*D*, *right panel*), indicating that excessive miR-143 did not confer an additional growth inhibitory effect on normal cells in which expression of miR-143 is maintained to a physiological level. This finding suggests that animal cells may have their own threshold amount for miRNA activity. The different sensitivity found in different cell types can help secretory miRNAs fulfill their purpose to combat exclusively precancerous cells. It is possible that secretory miRNAs, at least, derived from non-cancerous cells such as PNT-2 cells could supplement growth-suppressive signals that are decreased in cancerous cells. Thus, secreted miR-143 might be involved in the cell competitive regulatory system.

TABLE 1
A list of PNT-2-derived secretory miRNAs that were down-regulated less than 0.5-fold in PC-3M cells compared with PNT-2 cells

miRNAs	Fold change[a]
hsa-miR-141	0.0
hsa-miR-200c	0.0
hsa-miR-886–3p	0.0
hsa-miR-30a*	0.0
hsa-miR-155	0.0
hsa-miR-205	0.0
hsa-miR-224	0.0
hsa-miR-148a	0.0
hsa-miR-130a	0.0
hsa-miR-30a	0.1
hsa-miR-663	0.1
hsa-miR-181a-2*	0.1
hsa-miR-484	0.1
hsa-miR-10a	0.1
hsa-miR-192	0.1
hsa-miR-193b	0.1
hsa-miR-200a	0.1
hsa-miR-429	0.1
hsa-miR-769–5p	0.1
hsa-miR-200b	0.2
hsa-miR-195	0.2
hsa-miR-203	0.2
hsa-miR-7	0.2
hsa-miR-200a*	0.2
hsa-miR-200b*	0.2
hsa-miR-30c	0.2
hsa-miR-126	0.3
hsa-miR-149	0.3
hsa-miR-30d	0.3
hsa-miR-181a	0.3
hsa-miR-30e*	0.3
hsa-miR-365	0.4
hsa-miR-135b	0.4
hsa-miR-454*	0.4
hsa-miR-129*	0.4
hsa-miR-30b	0.4
hsa-miR-181b	0.4
hsa-miR-210	0.4
hsa-miR-455–3p	0.5
hsa-miR-15a	0.5

[a] Fold change of the expression of miRNAs in PC-3M cells compared with PNT-2 cells is indicated.

Secretory miR-143 Inhibited Prostate Cancer Cell Proliferation in Vitro—To examine whether miR-143 released from normal cells exert an anti-proliferative activity, we generated HEK293 cells overexpressing miR-143 by nearly 200-fold compared with control (supplemental Fig. 3*A*). After a 3-day incubation with the CM derived from the miR-143-overproducing HEK293 cells and control HEK293 cells, PC-3M-luc cells showed an ~50% decrease in proliferation (Fig. 3*A*, *lanes 1* and *3*). Importantly, the decrease was recovered by the transfection of anti-miR-143 in PC-3M-luc cells (Fig. 3*A*, *lane 3* and *4*). These data indicate that the growth inhibition is attributable to secretory miR-143 contained in the supernatant of miR-143-overexpressing HEK293 cells. In agreement with the exosome-dependent machinery of miRNA secretion, we observed a similar result by using exosome fractions purified from miR-143-transduced HEK293 cells (Fig. 3*B*).

To further study miRNA transfer on a molecular level, we performed a target gene expression analysis and an miRNA-responsive reporter assay. The immunoblotting analysis shows that the addition of the CM isolated from miR-143-overexpressing HEK293 cells significantly knocked down expression of KRAS, a target gene for miR-143 (21), in PC-3M-luc cells (Fig. 3*C*). In addition, we implemented luciferase analyses using

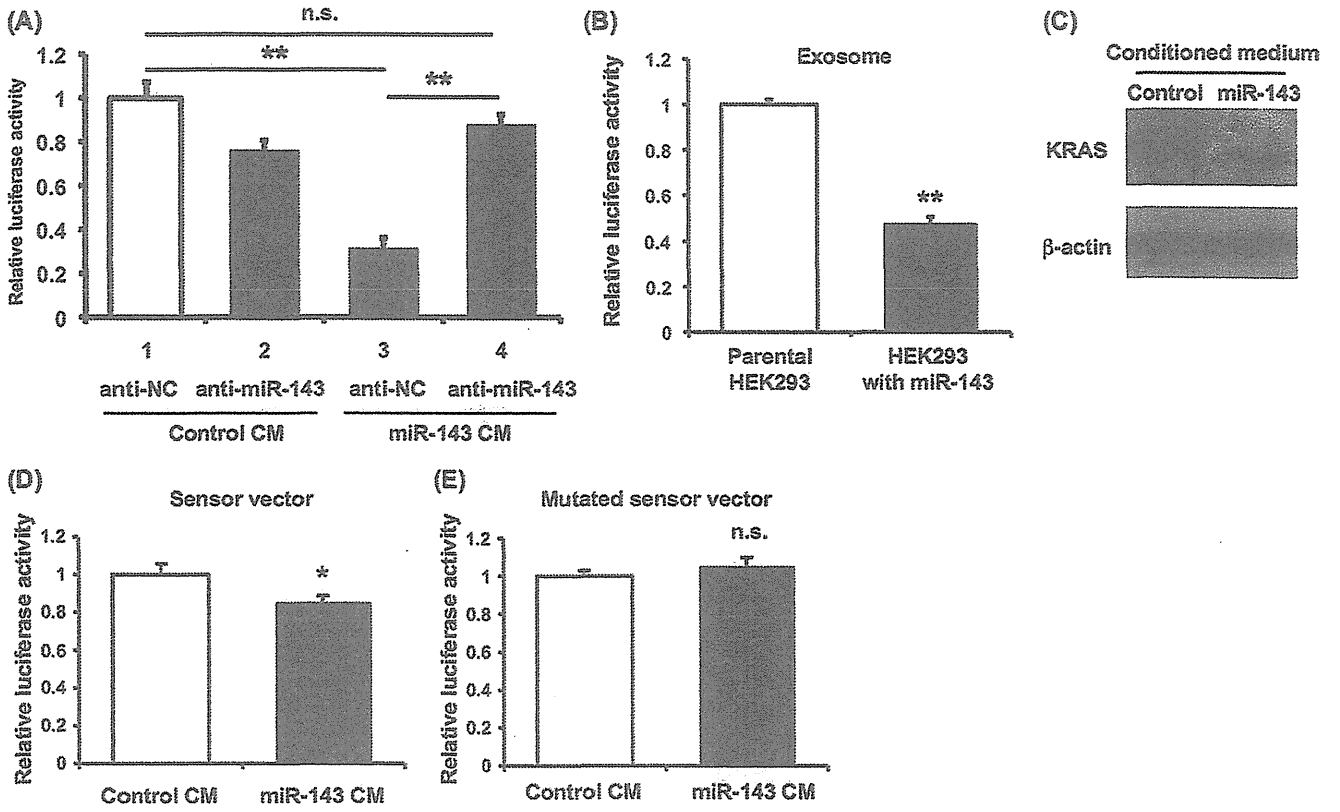

FIGURE 3. **Transfer of secretory miR-143 to PC-3M-luc cells *in vitro*.** *A*, the transfection of anti-miR-143 to PC-3M-luc cells restored the reduced cell growth by the CM derived from miR-143 overproducing cells. After the transfection with 3 nM miR-143 inhibitor molecule (anti-miR-143) (*lanes 2* and *4*) or its control molecule (*anti-NC*) (*lanes 1* and *3*), PC-3M-luc cells were incubated for 3 days in a control conditioned medium (*lanes 1* and *2*) and CM containing extracellular miR-143 (*lane 3* and *4*) followed by a cell growth assay as described under "Experimental Procedures." The values on the *y* axis are depicted relative to the normalized luciferase activity of cells treated in a culture medium, which is defined as 1. Each *bar* is presented as the mean S.E. ($n = 3$). (*, $p < 0.05$; Student's *t* test; *n.s.*, not significant). *B*, cell growth inhibition by exosomes derived from miR-143-transduced HEK293 cells is shown. PC-3M-luc cells were incubated in the exosomes followed by cell growth assay as described under "Experimental Procedures." The values on the *y* axis are depicted relative to the normalized luciferase activity of cells treated with exosomes derived from original HEK293 cells, defined as 1. Each *bar* is presented as the mean S.E. ($n = 3$). (**, $p < 0.005$; Student's *t* test). *C*, secretory miR-143-mediated KRAS suppression in PC-3M-luc cells is shown. Ten micrograms of protein of whole cell lysates prepared from PC-3M-luc cells treated with or without secretory miR-143 were applied to electrophoresis. Immunoblotting was performed with KRAS and actin antibodies and visualized by LAS-3000 system. *D*, extracellular miR-143 derived from HEK293 cells suppressed the luciferase activity of the sensor vector. HEK293 cells transfected with an miR-143 sensor vector were used as recipient cells. The recipient cells were incubated in a CM containing extracellular miRNAs. After a 2-day incubation, a luciferase reporter assay was performed as described under "Experimental Procedures." The values on the *y* axis are depicted relative to the normalized luciferase activity of original HEK293-conditioned medium-treated cells, which is defined as 1. Each *bar* is presented as the mean S.E. ($n = 3$). *, $p < 0.05$; Student's *t* test). *E*, extracellular miR-143 did not reduce the luciferase activity of the mutated sensor vector. HEK293 cells transfected with the mutated miR-143 sensor vector were used as recipient cells. The recipient cells were incubated in a conditioned medium containing extracellular miRNAs. The luciferase assay was carried out as described above. The values on the *y* axis are depicted relative to the normalized renilla luciferase activity of control cells, which is defined as 1. Each *bar* is presented as the mean S.E. ($n = 3$). *n.s.* represents not significant.

a sensor vector harboring renilla luciferase fused in tandem with miR-143 seed sequence in the 3′-UTR. As shown in Fig. 3*D*, the normalized renilla luciferase activities were reduced by the treatment of miR-143-enriched CM derived from HEK293 cells stably expressing miR-143. In contrast, we did not detect any changes of luminescence by using a mutated vector instead of the intact sensor vector (Fig. 3*E*). Furthermore, we quantified cellular amounts of miR-143 in PC-3M-luc cells incubated with CM derived from HEK293 cells or miR-143 overproducing HEK293 cells by QRT-PCR. As shown in supplemental Fig. 3*B*, miR-143 was clearly increased at a cellular level by the treatment of the miR-143 enriched CM. These results indicate that secretory miR-143 exhibits its on-target growth-inhibitory effect in neighboring precancerous cells, thereby suppressing their disordered growth.

Secretory miR-143 Functions as Tumor Suppressor in Vivo—To our knowledge it has never been demonstrated that extracellular tumor-suppressive miRNAs can be transferred into living cells and induce phenotypic change *in vivo*. To address this possibility, we injected CM derived from miR-143 overproducing HEK293 cells or parental HEK293 cells into nude mice implanted with PC-3M-luc cells. Four days after the subcutaneous implantation, we carried out *in vivo* imaging and CM injections according to the timetable shown in Fig. 4*A*. Tumor expansions have been restrained for 8 days with intratumor administrations of miR-143 enriched CM, and consequently the tumor masses shrank by ~0.5-fold on day 8 (Fig. 4*B*). The representative luminescent images of inoculated PC-3M-luc cells on day 8 were shown in Fig. 4*C*. Consistent with the finding that miR-143 did not impair growth activity of non-cancer cells *in vitro* (Fig. 2*D*), no toxicity was observed in these mice (data not shown). In addition, the expressions of miR-143 target genes, such as KRAS and ERK5 (16, 21), were decreased after miR-143-transduced CM injections, indicative of intercellular miRNA transfer *in vivo* (Fig. 4*D*). Thus, our prostate cancer xenograft model suggests that the tumor-suppressive miRNAs

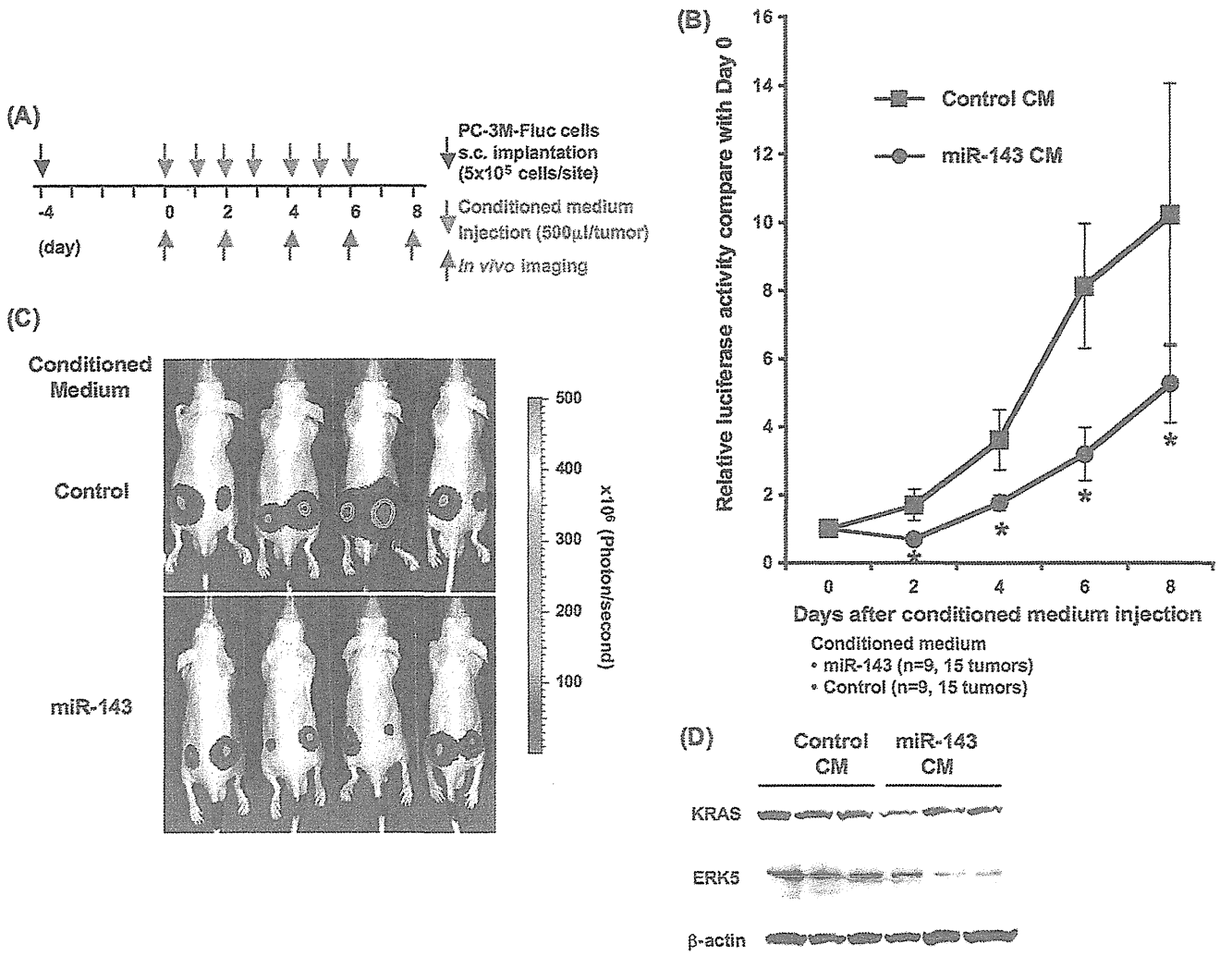

FIGURE 4. **Transfer of secretory miR-143 to PC-3M-luc cells *in vivo*.** *A*, shown is the timetable for conditioned medium injections and *in vivo* imaging. *B*, shown are tumor growth ratios of the inoculated PC-3M-luc cells during the secretory miR-143 treatment. *Closed circles* and *closed squares* indicate the tumor mass administrated with CM from miR-143-overproducing HEK293 cells or parental HEK293 cells, respectively. The values on the *y* axis are depicted relative to the luciferase activity of each tumor on day 0, which is defined as 1. Each *bar* is presented as the mean S.E. ($n = 9$). *, $p < 0.05$; Student's *t* test. *C*, representative images are shown of tumor cells in the skin of mice. Bioluminescence of firefly luciferase from miR-143-enriched CM treated mice and control mice were detected on day 8 with IVIS imaging system. *D*, shown is secretory miR-143-mediated KRAS and ERK5 suppression in inoculated tumor cells. On day 8 the inoculated tumor masses were isolated and applied to immunoblotting analysis for the quantification of KRAS and ERK5 on a protein level.

secreted from normal cells could be efficiently delivered into their neighboring tumors *in vivo*.

DISCUSSION

In this study we documented that miR-143 derived from non-cancerous cells had the ability to suppress the growth of cancer cell proliferation not only *in vitro* but also *in vivo*. These observations suggest that tumor-suppressive miRNAs can be implicated in cell competition between cancer cells and non-cancer cells. In this context, normal cells attempt to prevent the outgrowth of precancerous cells by secreting anti-proliferative miRNAs and maintain a healthy condition; however, the abnormal cells can circumvent this inhibitory machinery, finally resulting in a tumor expansion (Fig. 2*A*). Cell competition could be a homeostatic mechanism that tumor cells need to overcome (1).

Here, we discuss two possible mechanisms by which cancer cells can gain resistance to secretory tumor-suppressive miRNAs. One is a blockade for the uptake of miRNAs, and the other is a cancellation of silencing activity of the incorporated miRNAs. As previously reported, miRNAs are loaded into exosomes and then secreted from living cells (7, 22, 23). If exosomes enriched in miRNAs are actively incorporated by recipient cells, cancer cells can impair the uptake mechanism to escape from the attack of secretory tumor-suppressive miRNAs. This scenario is supported by a recent publication regarding a Tim4 expected for an exosome receptor (24).

In the latter case cancer cells need to specifically compromise the incorporated tumor-suppressive miRNAs because there are some types of miRNAs that are indispensable for the expansion of cancer cells. A RISC assembly is composed of many protein families, such as the mammalian AGO family, GW182, and heat shock proteins (25). Moreover, each gene family also consists of many members, thereby generating diversity of RISC assemblies. The heterogeneity of RISC assemblies allows tumor-suppressive miRNAs to selectively bind with a RISC and silence their target genes on the complex. If cancer cells can exclusively destroy the tumor-suppressive RISC assembly, they can safely

grow in a limited niche full of anti-proliferative miRNAs. The detailed mechanism of the resistance to cell competition remains unknown.

In addition to the acquired resistance, there is another possibility that normal cells will lose secretory capacity of exosomal miRNAs. p53 was shown to enhance exosome production in cells undergoing a p53 response to stress (26). In other words, dysfunction of p53 will result in decreased miRNA secretion. The tumor-suppressive ability of p53 can partly depend on the control of miRNA release from normal cells.

Numerous studies show a broad variety of reasons for tumor initiation, including gene amplification, cellular stress, metabolic alteration, and epigenetic changes. This work suggests that the disruption of the cell competitive process mediated by secretory miRNAs will result in the occurrence of neoplasm. Understanding the mechanism by which homeostasis is impaired leads to a novel therapeutic approach for cancer progression.

Acknowledgments—We thank Katsuyuki Hayashi and Ikuei Hiraka at DNA Chip Research Inc. for supporting the processing of microarray data. We thank Ayako Inoue for excellent technical assistance.

REFERENCES

1. Johnston, L. A. (2009) Competitive interactions between cells: death, growth, and geography. *Science* **324,** 1679–1682
2. Díaz, B., and Moreno, E. (2005) The competitive nature of cells. *Exp. Cell Res.* **306,** 317–322
3. Hanahan, D., and Weinberg, R. A. (2011) Hallmarks of cancer. The next generation. *Cell* **144,** 646–674
4. Bondar, T., and Medzhitov, R. (2010) p53-mediated hematopoietic stem and progenitor cell competition. *Cell Stem Cell* **6,** 309–322
5. Dong-Le Bourhis, X., Berthois, Y., Millot, G., Degeorges, A., Sylvi, M., Martin, P. M., and Calvo, F. (1997) Effect of stromal and epithelial cells derived from normal and timorous breast tissue on the proliferation of human breast cancer cell lines in co-culture. *Int. J. Cancer* **71,** 42–48
6. Senoo-Matsuda, N., and Johnston, L. A. (2007) Soluble factors mediate competitive and cooperative interactions between cells expressing different levels of *Drosophila* Myc. *Proc. Natl. Acad. Sci. U.S.A.* **104,** 18543–18548
7. Kosaka, N., Iguchi, H., Yoshioka, Y., Takeshita, F., Matsuki, Y., and Ochiya, T. (2010) Secretory mechanisms and intercellular transfer of microRNAs in living cells. *J. Biol. Chem.* **285,** 17442–17452
8. Croce, C. M. (2009) Causes and consequences of microRNA dysregulation in cancer. *Nat. Rev. Genet.* **10,** 704–714
9. Suzuki, H. I., Yamagata, K., Sugimoto, K., Iwamoto, T., Kato, S., and Miyazono, K. (2009) Modulation of microRNA processing by p53. *Nature* **460,** 529–533
10. Takeshita, F., Patrawala, L., Osaki, M., Takahashi, R. U., Yamamoto, Y., Kosaka, N., Kawamata, M., Kelnar, K., Bader, A. G., Brown, D., and Ochiya, T. (2010) Systemic delivery of synthetic microRNA-16 inhibits the growth of metastatic prostate tumors via down-regulation of multiple cell-cycle genes. *Mol. Ther.* **18,** 181–187
11. Peng, X., Guo, W., Liu, T., Wang, X., Tu, X., Xiong, D., Chen, S., Lai, Y., Du, H., Chen, G., Liu, G., Tang, Y., Huang, S., and Zou, X. (2011) Identification of miRs-143 and -145 that is associated with bone metastasis of prostate cancer and involved in the regulation of EMT. *PLoS One* **6,** e20341
12. Franses, J. W., Baker, A. B., Chitalia, V. C., and Edelman, E. R. (2011) *Sci. Transl. Med.* **3,** 66ra65
13. Savina, A., Vidal, M., and Colombo, M. I. (2002) The exosome pathway in K562 cells by Rab11. *J. Cell Sci.* **115,** 2505–2515
14. Trajkovic, K., Hsu, C., Chiantia, S., Rajendran, L., Wenzel, D., Wieland, F., Schwille, P., Brügger, B., and Simons, M. (2008) Ceramide triggers budding of exosome vesicles into multivesicular endosomes. *Science* **319,** 1244–1247
15. Gandellini, P., Folini, M., Longoni, N., Pennati, M., Binda, M., Colecchia, M., Salvioni, R., Supino, R., Moretti, R., Limonta, P., Valdagni, R., Daidone, M. G., and Zaffaroni, N. (2009) miR-205 exerts tumor-suppressive functions in human prostate through down-regulation of protein kinase Cepsilon. *Cancer Res.* **69,** 2287–2295
16. Clapé, C., Fritz, V., Henriquet, C., Apparailly, F., Fernandez, P. L., Iborra, F., Avancès, C., Villalba, M., Culine, S., and Fajas, L. (2009) miR-143 interferes with ERK5 signaling and abrogates prostate cancer progression in mice. *PLoS One* **4,** e7542
17. Kong, D., Li, Y., Wang, Z., Banerjee, S., Ahmad, A., Kim, H. R., and Sarkar, F. H. (2009) miR-200 regulates PDGF-D-mediated epithelial-mesenchymal transition, adhesion, and invasion of prostate cancer cells. *Stem Cells* **27,** 1712–1721
18. Fujita, Y., Kojima, K., Ohhashi, R., Hamada, N., Nozawa, Y., Kitamoto, A., Sato, A., Kondo, S., Kojima, T., Deguchi, T., and Ito, M. (2010) MiR-148a attenuates paclitaxel resistance of hormone-refractory, drug-resistant prostate cancer PC3 cells by regulating MSK1 expression. *J. Biol. Chem.* **285,** 19076–19084
19. Saito, Y., Friedman, J. M., Chihara, Y., Egger, G., Chuang, J. C., and Liang, G. (2009) Epigenetic therapy up-regulates the tumor suppressor microRNA-126 and its host gene EGFL7 in human cancer cells. *Biochem. Biophys. Res. Commun.* **379,** 726–731
20. Rauhala, H. E., Jalava, S. E., Isotalo, J., Bracken, H., Lehmusvaara, S., Tammela, T. L., Oja, H., and Visakorpi, T. (2010) miR-193b is an epigenetically regulated putative tumor suppressor in prostate cancer. *Int. J. Cancer* **127,** 1363–1372
21. Xu, B., Niu, X., Zhang, X., Tao, J., Wu, D., Wang, Z., Li, P., Zhang, W., Wu, H., Feng, N., Wang, Z., Hua, L., and Wang, X. (2011) miR-143 decreases prostate cancer cells proliferation and migration and enhances their sensitivity to docetaxel through suppression of KRAS. *Mol. Cell Biochem.* **350,** 207–213
22. Gibbings, D. J., Ciaudo, C., Erhardt, M., and Voinnet, O. (2009) Multivesicular bodies associate with components of miRNA effector complexes and modulate miRNA activity. *Nat. Cell Biol.* **11,** 1143–1149
23. Pegtel, D. M., Cosmopoulos, K., Thorley-Lawson, D. A., van Eijndhoven, M. A., Hopmans, E. S., Lindenberg, J. L., de Gruijl, T. D., Würdinger, T., and Middeldorp, J. M. (2010) Functional delivery of viral miRNAs via exosomes. *Proc. Natl. Acad. Sci. U.S.A.* **107,** 6328–6333
24. Miyanishi, M., Tada, K., Koike, M., Uchiyama, Y., Kitamura, T., and Nagata, S. (2007) Identification of Tim4 as a phosphatidylserine receptor. *Nature* **450,** 435–439
25. Kwak, P. B., Iwasaki, S., and Tomari, Y. (2010) The microRNA pathway and cancer. *Cancer Sci.* **101,** 2309–2315
26. Yu, X., Harris, S. L., and Levine, A. J. (2006) The regulation of exosome secretion. A novel function of the p53 protein. *Cancer Res.* **66,** 4795–4801

Breast Cancer Stem Cell: Translating to the Clinic

22

Makiko Ono, Yasuhiro Fujiwara, and Takahiro Ochiya

Abstract

Breast cancer is the most common cancer in women in both Western and Asian countries. Despite development of systemic chemotherapy, metastatic breast cancers are still incurable. Currently, evidence supports that a small subpopulation composed of cancer stem cells (CSCs) in a tumor can have self-renewing ability and tumorigenesis, and generate tumor to recapitulate a heterogeneous population of cancer cells in hierarchical fashion. Accordingly, CSC hypothesis brings a paradigm shift for breast cancer biology and treatment strategies. To elucidate how CSCs affect a person's risk and progression of breast cancer, many clinical trials for CSC-targeted therapeutics are ongoing.

Keywords

Breast cancer • Cancer stem cell • Circulating tumor cell • Notch • Wnt • Hedgehog

Introduction

Although the incidence of breast cancer is decreasing owing to screening and development of systemic therapy in Western countries, it is still the most common cancer in women. In Japan, the incidence of breast cancer is also the most frequent in women's cancer and is increasing due to westernization of life style and more than 45,000 women were newly diagnosed as breast cancer and more than 11,000 women died of breast cancer in 2007 (Center for Cancer Control and Information Services and National Cancer Center, Japan 2009). Despite development of systemic chemotherapy, advanced disease at diagnosis and recurrent disease which approximately one-third patients with early breast cancer develop are almost incurable. In such a case, response rates of systemic hormonal and chemotherapy are only 30–60%, and almost all of responded cancers

M. Ono • T. Ochiya (✉)
Division of Molecular and Cellular Medicine,
National Cancer Center Research Institute,
Tsukiji, Chuo-ku, Tokyo, Japan
e-mail: Tochiya@ncc.go.jp

Y. Fujiwara
Breast and Medical Oncology Division,
National Cancer Center Hospital,
Tsukiji, Chuo-ku, Tokyo, Japan

M.A. Hayat (ed.), *Stem Cells and Cancer Stem Cells, Volume 4*,
DOI 10.1007/978-94-007-2828-8_22,

regrow and show resistant to hormonal and chemotherapy. Thus, it is necessary to develop more effective treatment of breast cancer.

Over these 30 years, several hypotheses have been proposed in cancer progression. In 1976, the clonal evolution of tumor cell populations was proposed (Nowell 1976). Tumor heterogeneity was grown by random accumulation of genomic or epigenomic abnormalities and tumor cell population evolves by these stepwise genetic variations. By the stepwise genetic or epigenetic event, developmental clonal population which can acquire the sequential biological characteristics evolves, resulting in resistant to chemotherapy. On the other hand, the hypothesis had been also proposed that a small subpopulation in a tumor can have self-renewing ability and tumorigenesis, and generate tumor to recapitulate a heterogeneous population of cancer cells in hierarchical fashion (Wicha et al. 2006). The small subpopulation is called "tumor initiating cells" or "cancer stem cells (CSC)". In this CSC hypothesis, small subpopulation of CSCs, which is generally resistant to chemotherapy and radiation, has been already present before chemotherapy and proliferation of CSCs attributes to tumor regrowth during or after chemotherapy. In CSCs, resistance to cytotoxic chemotherapy and radiation, which usually target highly proliferating cells, is possibly due to their increased efficiency of DNA repair and alterations, their slow proliferation rate, or their high expression of adenosine triphosphate-binding cassette (ABC) transporters which are efflux pumps for many chemotherapeutic drugs. Accordingly, it is has been suggested that strategy that targeting CSCs is needed to cure breast cancer, and thus elucidating characteristics of CSCs with regulatory molecular pathways or their markers is important for further clinical implication.

Since recent development of flow cytometric sorting enables researchers to detect and isolate cells expressing specific cell surface markers in cell lines and clinical specimens of various tumors, CSC hypothesis becomes more evident and dominant compared with clonal selection. After CSCs were first identified in human acute myeloid leukemia that showed ability to form tumors in immunodeficient mice (Lapidot et al. 1994), they were also characterized in solid tumors including breast, colon, lung, prostate, brain, pancreatic, and head and neck cancer, and multiple myeloma (Visvader and Lindeman 2008). In this chapter, we focus on current development and controversies in breast CSCs.

Markers of Breast Cancer Stem Cells

Breast CSCs were characterized by the expression of CD44 and low or no expression of CD24 (Al-Hajj et al. 2003). They showed that as few as 100 cancer cells with $CD44^+/CD24^-$ phenotype from pleural effusion in patients with breast cancer were capable of forming tumors in NOD/SCID mice, whereas cancer cells without $CD44^+/CD24^-$ phenotype were unable to generate tumors when 10^5 cells were implanted into same kind of mice. In addition, the tumorigenic subpopulation was able to be passaged and regenerate mixed subpopulation composed of both tumorigenic and non-tumorigenic cells same as the initial tumor. Consequently, tumorigenic cells of breast cancer were isolated and propagated in vitro, and the 95–98% of cells in the culture revealed $CD44^+/CD24^-$ phenotype by flow-cytometric analysis (Ponti et al. 2005). In addition, 10–20% of $CD44^+/CD24^-$ cells maintained the ability to self-renewal with establishment of secondary spheres and other cell types which were not capable of self-renewal were also encompassed. Taken together, CSC properties of $CD44^+/CD24^-$ cells in breast cancer were revealed in vitro.

As another marker of breast CSCs, ALDH1 (aldehyde dehydrogenase-1) has been also reported (Ginestier et al. 2007). It was revealed that ALDH1 was a cell surface marker of both normal and malignant mammary stem cells and predicted poor prognosis in breast cancer patients in 2007. Cell population having ALDH enzymatic activity, which was defined as ALDEFLUOR-positive cells in the study, composed of approximately 8% in normal mammary epithelial cells. It was capable of generating mammospheres in suspension culture and being passaged several times. In addition, 5,000 ALDEFLUOR-positive cells from normal mammary epithelium could have outgrowth

potential with duct formation, when transplanted into mammary fat pads of NOD/SCID mice. On the other hand, ALDEFLUOR-negative cells could not either generate spheres or generate epithelial outgrowth, even when 50,000 cells were implanted. Similarly, ALDEFLUOR-positive population represented 3–10% in invasive ductal carcinomas, and only 500 ALDEFLUOR-positive cells could form tumors and recapitulate the heterogeneity of the initial tumor when transplanted orthotopically in the fat-pad of NOD/SCID mice.

Clinical Relevance of CSC Markers in Breast Cancer

Using clinical specimens of breast cancer, many researchers reported clinical relevance of cell markers of CSCs described above. In 2005, it was reported that $CD44^+/CD24^{-/low}$ cancer cells did not increase according to a stepwise breast cancer progression from carcinoma in situ to invasive carcinoma (Abraham et al. 2005). In addition, there were no significant association between prevalence of $CD44^+/CD24^{-/low}$ cancer cells and clinicopathological characteristics. Although patients with high percentage of $CD44^+/CD24^{-/low}$ cancer cells significantly had higher incidence of distant metastasis, there were no significant difference in disease-free survival and overall survival between tumors with high and low percentage of $CD44^+CD24^{-/low}$ cancer cells. On the other hand, genetic signatures from $CD44^+/CD24^-$ cancer cells were reported to be correlated with metastasis-free survival and overall survival (Liu et al. 2007).

It was reported relationship between change in percentage of $CD44^+/CD24^{-/low}$ cells in breast cancer and the effect of chemotherapy (Li et al. 2008). They tested the proportion of $CD44^+/CD24^{-/low}$ cells by flow cytometry and mammosphere-forming efficiency (MSFE) before and after conventional chemotherapy or lapatinib, a dual tyrosine kinase inhibitor targeting epidermal growth factor receptor (EGFR) and HER2 receptor. Conventional chemotherapy significantly increased both the percentage of $CD44^+/CD24^{-/low}$ cells and MSFE, whereas lapatinib decreased the percentage of $CD44^+/CD24^{-/low}$ cells and MSFE. It was also revealed that the molecular profile of residual tumors obtained after chemotherapy closely resembled the gene expression profile of $CD44^+/CD24^-$ and mammosphere-forming cells (Creighton et al. 2009). The gene profile is also expressed in claudin-low subtype of breast cancers that is thought to be resistant to conventional chemotherapy. These results revealed clinical evidence that tumorigenetic $CD44^+/CD24^{-/low}$ subpopulation in breast cancer was intrinsically resistant to conventional chemotherapy.

Similarly, there is controversial data for clinical significance of ALDH1 in breast cancer (Resetkova et al. 2010). Although CSC hypothesis may be definite, there are many unresolved questions for clinical relevance of CSC markers of $CD44^+/CD24^{-/low}$ and ALDH1. Small sample size, imbalance in clinical factors and different methodologies partly cause contradictory results. Standardization of methodologies, studies with large sample size and balanced clinical factors are needed.

CSCs and Breast Cancer Subtypes

The heterogeneous nature of breast cancer has been demonstrated by gene expression profiling using the DNA microarray technique (Perou et al. 2000). Genetically, invasive breast cancers have been classified into at least six subtypes, comprising luminal A, luminal B, ERBB2 (HER2), basal-like, claudin-low, and normal breast-like subtypes, which demonstrate characteristic immunohistochemical features and clinical behavior such as response to chemotherapeutic agents, metastatic pattern and prognosis.

It is suggested that human breast cancer may arise from the transformation of either mammary stem cells or early progenitor cells leading to produce distinct subtypes of breast cancers (Li et al. 2003; Wicha et al. 2006). In addition, as shown in researches of transgenic mouse model of mammary tumorigenesis, distinct oncogenes and molecular pathways affect different stem and progenitor cells, resulting in heterogeneity in breast cancers. Actually, luminal progenitor cells were reported to be represented a probable cancer initiating cells in *BRCA1* mutation carriers who developed basal-like breast cancers, and suggested that

mammary SCs (MaSCs) and luminal progenitors are the cells of origin of claudin-low and basal-like tumors, respectively (Lim et al. 2009). Based on the study, Prat and Perou described relationship between breast cancer subtypes and MaSCs and progenitor cells which the subtypes may originate from, and suggested the existence of multiple cell-of-origin (Prat and Perou 2009). That is, the molecular classifications of human breast cancers by gene expression analysis may reflect different cellular origins and affected genes. Hereafter, therapeutics targeting specific cell-of-origin in each breast cancer subtype will be expected. Until now, however, there has been few clinical data that shows association between distinct breast cancer subtypes and their cell-of-origin with specific markers. It is possible that $CD44^{+}/CD24^{-/low}$ and ALDH1 could not represent cancer stem/progenitor cells in all subtypes of breast cancer, as demonstrated by Lim et al. in which flow cytometry of EpCAM and CD49f expression was used to isolate MaSCs and progenitor cells (Lim et al. 2009). That may be the reason why discrepant results of clinical data have been reported, as previously mentioned. Development of markers for breast CSCs is also needed to elucidate clinical relevance of CSCs in different breast cancer subtypes.

CSCs and Circulating Tumor Cells

Metastases, which unable almost of cancer patients to cure, necessitate that tumor cells in a primary site invade the surrounding tissue, enter the microvasculature, translocate surviving through bloodstream or lymphatic, extravasate and survive in the microenvironment of distant tissues, leading to formation of a macroscopic tumor. Therefore, circulating tumor cells (CTCs) are crucial process to tumor dissemination. Actually, CTCs are reported to be a negative prognostic factor regardless of other prognostic factors in metastatic breast cancer (Mego et al. 2010). In addition, it is speculated that CTCs have stem cell properties. In the study examining CTCs with AdnaTest in 39 patients with metastatic breast cancer patients, CTC was detected in 31% of clinical blood samples and response to systemic therapy was worse in CTC-positive patients compared to those without CTC. In addition, 69% of CTC-positive samples were positive for ALDH1. In another study, 16 of 20 metastatic breast cancer patients had CTCs examined by CellSearch system, and HER2 and Notch1 was expressed in 63% and 67% of patients positive for CTCs, respectively, whereas HER2 expression of primary tumors was positive in 22% of CTC-positive patients (Mego et al. 2010). In addition, HER2 and Notch1 expression were significantly correlated. Taken together, although CTCs seem to be associated with stem cell phenotype, technical improvement in detection methods of CTCs is needed.

Molecular Pathways in Breast Cancer Stem Cells

Developmental signaling pathways including Notch, Hedgehog, and Wnt have been showed to play a critical role in regulating the self-renewal of mammary, hematopoietic, and neuronal stem cells. In CSC hypothesis, it is likely that dysregulation of their pathways contributes to generate tumors driven by cells with stem cell properties. Actually, a number of evidence that supports this speculation in vitro and in vivo has been reported, and clinical trials that test whether controlling their pathways could prevent breast cancer recurrence or improve clinical prognosis has been started yet. We describe major pathways which have been reported regarding breast CSCs; Notch pathway, Wnt pathway, and Hedgehog pathway.

Notch Pathway

Notch receptor and ligand are composed of four type1 transmembrane receptors (Notch 1–4) and five transmembrane ligands [delta ligand-like (DLL) 1, 3, and 4, and jagged (JAG) 1 and 2] (Ranganathan et al. 2011). Ligands expressed in the signal-sending cell bind to the extracellular domain (ECD) of Notch receptors on the signal-receiving cell. That causes a conformational

change by which the A disintegrin and metallopeptidase 10 or 17 (ADAM10/17) acts on the S2 cleavage site in the ECD. Consequently, gamma secretase enzymes mediate S3 cleavage, resulting in translocation of ICD from membrane into the nucleus. And then, ICD in the nucleus forms a complex with the RBPJ/CSL and MAML and the complex activates transcription of downstream target genes. Notch signal plays an important role in regulating cell fate, apoptosis, proliferation, and migration in normal breast development and is thought to be implicated in breast cancer initiation and progression. In addition, although detailed mechanisms are not completely realized, each Notch receptor seems to play distinct roles in the progression of different breast cancer subtypes. Notch4 is overexpressed more frequently in triple-negative breast cancers compared with other breast cancer subtypes. Notch3 plays a crucial role in the proliferation of HER2-negative breast cancers, but not HER2-positive breast cancers.

Notch signaling was showed to be frequently activated in breast cancers and sufficient to transform normal breast epithelial cells through suppression of apoptosis (Stylianou et al. 2006). Notch4 receptor is expressed in the stem cells of the normal breast epithelium and inhibition of the receptor leads to reduce stem cell activity. Similarly, Notch gene highly expresses in breast CSC subpopulation. For example, in ductal carcinoma in situ (DCIS) which has a great mammosphere-forming ability (MFE), the levels of NICD were increased and blocking Notch activity by a gamma-secretase inhibitor (GSI) or neutralizing antibody to Notch4 repressed DCIS MFE (Farnie et al. 2007). In addition, NICD-positive DCIS was significantly poor clinical outcome compared with NICD-negative DCIS. Taken together, Notch signaling pathway is directly involved in breast CSCs and it is suggested that targeting Notch signaling may improve breast cancer prognosis.

Wnt Pathway

Wnt (wingless-type MMTC integration site family) are cysteine-rich, secreted glycoproteins involved in controlling the processes of embryonic development regarding cell proliferation, differentiation, and development of normal breast tissues. Wnt ligands bind to the membrane frizzled receptors and to low density lipoprotein receptor-related protein (LRP), leading to release of β-catenin from complex composed of several proteins including Axin1/2, adenomatosis polyposis coli (APC) and glycogen synthase kinase (GSK) – 3β. As a result, unphosphorylated β-catenin accumulates in the cytoplasm and translocates into the nucleus, leading to regulation of the expression of target genes. Transgenic expression of genes involved in Wnt signaling pathway induced to mammary hyperplasia and early tumor progression (Li et al. 2003). In addition, induced mammary tumors contain increased fraction of mammary stem cells and/or progenitor cells which are likely to give rise to transformed cells, and thus oncogenesis by Wnt signaling targets mammary stem cells and/or progenitor cells which are major determinant of tumor susceptibility. In breast cancers, it is reported that uncomplexed transcriptionally active form of β- catenin is upregulated without mutations afflicting downstream components (Verkaar and Zaman 2011). There are many reports for inactivation of negative regulators and activation of positive regulators in Wnt signaling pathway in breast cancer. Expression of Frizzled-related protein 1 (Frp1), a secreted Wnt inhibitor, is either repressed or absent in approximately 80% of breast cancers. Dishevelled (Dvl), involved in Wnt signal transduction process, is amplified and upregulated in approximately 50% of breast ductal carcinomas.

Hedgehog Pathway

Hedgehog signaling has been reported to be active during mammalian development and regulate self-renewal of stem cell in normal breast tissues (Merchant and Matsui 2010). Hedgehog pathway begins to be activated, when one of three ligands composed of Sonic (SHh), Desert (DHh) and Indian Hedgehog (IHh) binds to Patched (Ptch1) which is a 12-pass transmembrane-spanning receptor and represses Smoothened

(Smo). Ligand binding to Ptch allows Smo to be derepressed and Gli transcription factors are processed to activating forms, leading to induce the transcription of Hedgehog target genes. Hedgehog signaling in cancer is activated by mutations in Hedgehog-related genes, ligand-mediated autocrine, or ligand-mediated paracrine and seems to function dependent on distinct biological and clinical factors, and each tumor type. In breast cancer, Hedgehog signaling is activated by both autocrine and paracrine. In addition, in breast CSCs defined as $CD44^+CD24^{-/low}lin^-$ by flow cytometry, increase in expression of PTCH1, Gli1, and Gli2, which was also seen in normal human mammary stem/progenitor cells, showed that Hedgehog signaling was activated (Liu et al. 2006). Using GLI1-overexpresing transgenic model, Gli1 expression was showed to induce cell proliferation and hyperplastic lesions and tumors develope in mammary gland with overexpression of Gli1 (Fiaschi et al. 2009).

Therapeutic Implications

According to CSC hypothesis, there may be at least two separate subpopulations with CSCs and non-CSCs in cancer cells. CSCs, which have self-renewal ability but lower proliferation rate and comprise quite a low percentage of tumor cells, are resistant to conventional cytotoxic agents and radiation. On the other hand, non-CSCs, which have no self-renewing potential but higher proliferation rate and account for the bulk of tumor cells that cause clinical symptoms and deterioration of visceral function in advanced disease, are susceptible to cytotoxic chemotherapeutic agents. Based on this concept, not only CSC-targeted monotherapy but also combination therapy that separately targets CSCs and non-CSCs is proposed. Eradication of CSCs could prevent treatment resistance and tumor recurrence, resulting in cure, whereas to eliminate non-CSCs contributes to shrinkage of bulk of tumors and high response rates, leading to relieve from main problems especially in patients with advanced disease. Although there is no definite clinical data showing effectiveness of CSC-targeted therapy, laboratory studies suggest several potential candidates, such as molecules targeting Notch, Hedgehog, and Wnt pathways. Some early phase trials which have been already reported until now are described below, and ongoing clinical trials are shown in Table 22.1. All of the trials are phase I or II trials.

In Notch signaling pathway, several GSIs and anti-Notch4 receptor antibodies are clinically under investigation. It was reported that a phase Ib trial of GSI, MK-0752 followed by docetaxel in patients with locally advanced or metastatic breast cancer refractory to anthracycline (Schott et al. 2010). In enrolled 30 patients, toxicities were well tolerated and response rate was 45%. $CD44^+/CD24^-$ cell population was significantly fewer in biopsies after treatment compared to baseline biopsies. Is was also studied that a pilot study of MK-0752 added to ongoing endocrine therapy with tamoxifen or letrozole in patients with estrogen receptor α- positive, early stage breast cancer in neoadjuvant setting (Albain et al. 2010). All tumors showed significant biomarker response with Ki67, Notch4, and NOXA, and toxicities were feasible. Gene expression level of Notch4 was significantly decreased after combination therapy and correlated strongly with Ki67 decrease of gene expression level.

In Hedgehog signaling pathway, Smo antagonists have been developed in several pharmaceutical companies. A phase I study of LDE225 in 31 patients with advanced solid tumors showed well tolerability and mild efficacy with partial response in one medulloblastoma and long stable disease in several solid tumors including breast cancer (Ahnert et al. 2010). A phase I trials of another Smo antagonists in monotherapy and combination therapy are ongoing, shown in Table 22.1.

As another therapeutic agent, metformin, an oral hypoglycemic agent, selectively targets breast CSCs despite an unclear mechanism (Hirsch et al. 2009). In addition, metformin combined with doxorubicin killed both CSCs and non-CSCs in culture and effectively reduced tumor mass in a xenograft model. In a study of

Table 22.1 Ongoing clinical trials targeting Notch, Hedgehog and Wnt signalings in patients with breast cancer

Target	Agent	Mechanism of action	Phase	Regimen	Patients
Notch	MK0752	γ-secretase inhibitor	I	MK0752	Advanced BC
			I	MK0752 + Tamoxifen or Letrozole	Early, ER (+) BC, neoadjuvant setting
			I	MK0752 + Ridaforolimus	Advanced tumors
			I	MK0752 + Dalotuzumab	Advanced tumors
			I/II	MK0752 followed by Docetaxel	Advanced or metastatic BC
	RO4929097	γ-secretase inhibitor	II	RO4929097	Advanced, metastatic or recurrent BC
			I	RO4929097 + Cediranib Maleate	Advanced solid tumors
			I	RO4929097 + Capecitabine	Refractory solid tumors
			I	RO4929097 + Gemcitabine	Advanced solid tumors
			I	RO4929097 + Paclitaxel + Carboplatin	Stage II or III triple negative BC, neoadjuvant setting
			I	RO4929097 + Temsirolimus	Advanced solid tumors
			I/II	RO4929097 + Exemestane	Pre/postmenopausal, advanced or metastatic BC
			I/II	RO4929097 + WBRT or SRS	BC with brain metastases
			II	RO4929097 + Letrozole	Postmenopausal, HR (+), stage II or III BC
Hedgehog	PF-04449913	SMO antagonist	I	PF-04449913	Solid tumors
	GDC-0449	SMO antagonist	I	GDC-0449	Locally advanced or metastatic solid tumors
Notch + Hedgehog	GDC-0449 RO4929097	SMO antagonist + γ-secretase inhibitor	I	GDC-0449 + RO4929097	Advanced BC
Wnt	PRI-724	CBP/β-catenin inhibitor	I	PRI-724	Advanced solid tumors

Abbreviations: *BC* breast cancer, *ER* estrogen receptor, *WBRT* whole brain radiation therapy, *SRS* stereotactic radiosurgery, *HR* hormone receptor

2,529 patients receiving neoadjuvant chemotherapy, pathological complete response rate (pCR) was significantly higher in diabetic patients treated with metformin than non-diabetic and diabetic patients without metformin (Jiralerspong et al. 2009). More than five clinical trials of metformin in combination with cytotoxic or molecular targeted agents in patients with early and metastatic breast cancer are ongoing.

Conclusions

Owing to development of biotechnology, we can elucidate molecular pathways and their interactions in cancer biology. Although precise mechanisms in tumorigenesis and tumor progression are not completely recognized, new knowledge introduces another approach to cancer treatment of CSC-targeted therapy. Simultaneously, CSC hypothesis also gives us significant implication for cancer risk estimation, early detection, prognostication, and prevention.

We certainly enter a new era in cancer treatment. Although therapeutics based on CSC hypothesis have not yet found effective, further research for CSCs will enable us to achieve improvement of clinical outcome in cancer patients.

Acknowledgements This work was supported in part by a Grant-in-aid for the Third-Term Comprehensive 10-Year Strategy for Cancer Control, the Program for Promotion of Fundamental Studies in Health Sciences of the National Institute of Biomedical Innovation (NiBio), and the Japan Society for the Promotion of Science (JSPS) through the "Funding Program for World-Leading Innovative R&D on Science and Technology (FIRST Program)," initiated by the Council for Science and Technology Policy (CSTP).

References

Abraham BK, Fritz P, McClellan M, Hauptvogel P, Athelogou M, Brauch H (2005) Prevalence of CD44+/CD24−/low cells in breast cancer may not be associated with clinical outcome but may favor distant metastasis. Clin Cancer Res 11:1154–1159

Ahnert JR, Baselga J, Tawbi HA, Shou Y, Granvil C, Dey J, Mita AC, Thomas AL, Amakye DD, Mita AC (2010) A phase I dose-escalation study of LDE225, a smoothened (Smo) antagonist, in patients with advanced solid tumors. J Clin Oncol 28:15s: abstract 2500

Al-Hajj M, Wicha MS, Benito-Hernandez A, Morrison SJ, Clarke MF (2003) Prospective identification of tumorigenic breast cancer cells. Proc Natl Acad Sci USA 100:3983–3988

Albain KS, Czerlanis C, Rajan P, Zlobin A, Godellas C, Bova D, Lo SS, Robinson P, Sarker S, Gaynor ER, Cooper R, Aranha G, Czaplicki K, Busby B, Rizzo P, Chisamore M, Demuth T, Blackman S, Watters J, Stiff P, Fuqua SAW, Miele L (2010) Combination of notch inhibitor MK-0752 and endocrine therapy for early stage ERα+Breast cancer in a presurgical window pilot study. Cancer Res 70(24 Suppl): Abstract nr PD05-12

Center for Cancer Control and Information Services and National Cancer Center, Japan (2009) Vital statistics Japan. Ministry of Health, Labour and Welfare

Creighton CJ, Li X, Landis M, Dixon JM, Neumeister VM, Sjolund A, Rimm DL, Wong H, Rodriguez A, Herschkowitz JI, Fan C, Zhang X, He X, Pavlick A, Gutierrez MC, Renshaw L, Larionov AA, Faratian D, Hilsenbeck SG, Perou CM, Lewis MT, Rosen JM, Chang JC (2009) Residual breast cancers after conventional therapy display mesenchymal as well as tumor-initiating features. Proc Natl Acad Sci USA 106:13820–13825

Farnie G, Clarke RB, Spence K, Pinnock N, Brennan K, Anderson NG, Bundred NJ (2007) Novel cell culture technique for primary ductal carcinoma in situ: role of Notch and epidermal growth factor receptor signaling pathways. J Natl Cancer Inst 99:616–627

Fiaschi M, Rozell B, Bergstrom A, Toftgard R (2009) Development of mammary tumors by conditional expression of GLI1. Cancer Res 69:4810–4817

Ginestier C, Hur MH, Charafe-Jauffret E, Monville F, Dutcher J, Brown M, Jacquemier J, Viens P, Kleer CG, Liu S, Schott A, Hayes D, Birnbaum D, Wicha MS, Dontu G (2007) ALDH1 is a marker of normal and malignant human mammary stem cells and a predictor of poor clinical outcome. Cell Stem Cell 1:555–567

Hirsch HA, Iliopoulos D, Tsichlis PN, Struhl K (2009) Metformin selectively targets cancer stem cells, and acts together with chemotherapy to block tumor growth and prolong remission. Cancer Res 69:7507–7511

Jiralerspong S, Palla SL, Giordano SH, Meric-Bernstam F, Liedtke C, Barnett CM, Hsu L, Hung MC, Hortobagyi GN, Gonzalez-Angulo AM (2009) Metformin and pathologic complete responses to neoadjuvant chemotherapy in diabetic patients with breast cancer. J Clin Oncol 27:3297–3302

Lapidot T, Sirard C, Vormoor J, Murdoch B, Hoang T, Caceres-Cortes J, Minden M, Paterson B, Caligiuri MA, Dick JE (1994) A cell initiating human acute myeloid leukaemia after transplantation into SCID mice. Nature 367:645–648

Li X, Lewis MT, Huang J, Gutierrez C, Osborne CK, Wu MF, Hilsenbeck SG, Pavlick A, Zhang X, Chamness GC, Wong H, Rosen J, Chang JC (2008) Intrinsic

resistance of tumorigenic breast cancer cells to chemotherapy. J Natl Cancer Inst 100:672–679

Li Y, Welm B, Podsypanina K, Huang S, Chamorro M, Zhang X, Rowlands T, Egeblad M, Cowin P, Werb Z, Tan LK, Rosen JM, Varmus HE (2003) Evidence that transgenes encoding components of the Wnt signaling pathway preferentially induce mammary cancers from progenitor cells. Proc Natl Acad Sci USA 100:15853–15858

Lim E, Vaillant F, Wu D, Forrest NC, Pal B, Hart AH, Asselin-Labat ML, Gyorki DE, Ward T, Partanen A, Feleppa F, Huschtscha LI, Thorne HJ, Fox SB, Yan M, French JD, Brown MA, Smyth GK, Visvader JE, Lindeman GJ (2009) Aberrant luminal progenitors as the candidate target population for basal tumor development in BRCA1 mutation carriers. Nat Med 15:907–913

Liu R, Wang X, Chen GY, Dalerba P, Gurney A, Hoey T, Sherlock G, Lewicki J, Shedden K, Clarke MF (2007) The prognostic role of a gene signature from tumorigenic breast-cancer cells. N Engl J Med 356:217–226

Liu S, Dontu G, Mantle ID, Patel S, Ahn NS, Jackson KW, Suri P, Wicha MS (2006) Hedgehog signaling and Bmi-1 regulate self-renewal of normal and malignant human mammary stem cells. Cancer Res 66:6063–6071

Mego M, Mani SA, Cristofanilli M (2010) Molecular mechanisms of metastasis in breast cancer – clinical applications. Nat Rev Clin Oncol 7:693–701

Merchant AA, Matsui W (2010) Targeting Hedgehog – a cancer stem cell pathway. Clin Cancer Res 16:3130–3140

Nowell PC (1976) The clonal evolution of tumor cell populations. Science 194:23–28

Perou CM, Sorlie T, Eisen MB, van de Rijn M, Jeffrey SS, Rees CA, Pollack JR, Ross DT, Johnsen H, Akslen LA, Fluge O, Pergamenschikov A, Williams C, Zhu SX, Lonning PE, Borresen-Dale AL, Brown PO, Botstein D (2000) Molecular portraits of human breast tumours. Nature 406:747–752

Ponti D, Costa A, Zaffaroni N, Pratesi G, Petrangolini G, Coradini D, Pilotti S, Pierotti MA, Daidone MG (2005) Isolation and in vitro propagation of tumorigenic breast cancer cells with stem/progenitor cell properties. Cancer Res 65:5506–5511

Prat A, Perou CM (2009) Mammary development meets cancer genomics. Nat Med 15:842–844

Ranganathan P, Weaver KL, Capobianco AJ (2011) Notch signalling in solid tumours: a little bit of everything but not all the time. Nat Rev Cancer 11:338–351

Resetkova E, Reis-Filho JS, Jain RK, Mehta R, Thorat MA, Nakshatri H, Badve S (2010) Prognostic impact of ALDH1 in breast cancer: a story of stem cells and tumor microenvironment. Breast Cancer Res Treat 123:97–108

Schott AF, Chang JC, Krop IE, Griffith KA, Layman RM, Hayes DF, Wicha MS (2010) Phase Ib Trial of the Gamma Secretase Inhibitor (GSI), MK-0752 followed by docetaxel in locally advanced or metastatic breast cancer. Cancer Res 70(24 Suppl): Abstract nr P6-15-03

Stylianou S, Clarke RB, Brennan K (2006) Aberrant activation of notch signaling in human breast cancer. Cancer Res 66:1517–1525

Verkaar F, Zaman GJ (2011) New avenues to target Wnt/beta-catenin signaling. Drug Discov Today 16:35–41

Visvader JE, Lindeman GJ (2008) Cancer stem cells in solid tumours: accumulating evidence and unresolved questions. Nat Rev Cancer 8:755–768

Wicha MS, Liu S, Dontu G (2006) Cancer stem cells: an old idea – a paradigm shift. Cancer Res 66:1883–1890; discussion 1895–1886

HUMAN GENE THERAPY 23:173–186 (February 2012)

DOI: 10.1089/hum.2011.046

Syngeneic Hematopoietic Stem Cell Transplantation Enhances the Antitumor Immunity of Intratumoral Type I Interferon Gene Transfer for Sarcoma

Takeshi Udagawa,[1,2] Kenta Narumi,[1] Naoko Goto,[1] Kouichirou Aida,[1] Koji Suzuki,[1] Takahiro Ochiya,[3] Atsushi Makimoto,[4] Teruhiko Yoshida,[5] Tatsuya Chikaraishi,[2] and Kazunori Aoki[1]

Abstract

Sarcoma at advanced stages remains a clinically challenging disease. Interferons (IFNs) can target cancer cells by multiple antitumor activities, including the induction of cancer cell death and enhancement of immune response. However, the development of an effective cancer immunotherapy is often difficult, because cancer generates an immunotolerant microenvironment against the host immune system. An autologous hematopoietic stem cell transplantation (HSCT) is expected to reconstitute a fresh immune system, and expand tumor-specific T cells through the process of homeostatic proliferation. Here we examined whether a combination of autologous HSCT and IFNs could induce an effective tumor-specific immune response against sarcoma. First, we found that a type I IFN gene transfer significantly suppressed the cell growth of various sarcoma cell lines, and that IFN-β gene transfer was more effective in inducing cell death than was IFN-α in sarcoma cells. Then, to examine the antitumor effect *in vivo*, human sarcoma cells were inoculated in immune-deficient mice, and a lipofection of an IFN-β-expressing plasmid was found to suppress the growth of subcutaneous tumors significantly. Finally, the IFN gene transfer was combined with syngeneic HSCT in murine osteosarcoma models. Intratumoral IFN-β gene transfer markedly suppressed the growth of vector-injected tumors and inhibited formation of spontaneous lung and liver metastases in syngeneic HSCT mice, and an infiltration of many immune cells was recognized in metastatic tumors of the treated mice. The treated mice showed no significant adverse events. A combination of intratumoral IFN gene transfer with autologous HSCT could be a promising therapeutic strategy for patients with sarcoma.

Introduction

PRIMARY MALIGNANT BONE TUMORS are rare, accounting for only 0.2% of all new cases of cancer. Osteosarcoma is the most common primary bone tumor with a peak incidence corresponding to the normal skeletal growth spurt of adolescence. Although complete surgical excision is most important for prognosis, the use of intensive neoadjuvant and adjuvant chemotherapy has improved survival (Link *et al.*, 1986; Longhi *et al.*, 2006). Relapse-free survival rates have improved from less than 20% without chemotherapy to 55–70% with a combination of surgery and multiagent chemotherapy. However, a significant proportion of patients develop recurrent disease, most commonly in the lungs, and the overall survival of patients with advanced osteosarcoma remains dismal (Bacci *et al.*, 2005; Chou *et al.*, 2005; Kempf-Bielack *et al.*, 2005).

Soft-tissue sarcoma also represents a rare entity of malignant tumors of various histologies. The cure of early disease depends on the appropriate multidisciplinary therapy of the primary tumor, including surgery and radiotherapy (Sarcoma Meta-analysis Collaboration, 1997). Adjuvant chemotherapy has not been shown to improve overall survival significantly, and chemotherapeutic interventions in metastatic soft-tissue sarcoma were generally disappointing (Borden *et al.*, 1990; Antman, 1997). New therapeutic approaches are needed in the therapeutic strategy of malignant bone and soft-tissue sarcoma.

[1]Division of Gene and Immune Medicine, National Cancer Center Research Institute, Tokyo 104-0045, Japan.
[2]Department of Urology, St. Marianna University, Kanagawa 216-8511, Japan.
[3]Division of Molecular and Cellular Medicine, National Cancer Center Research Institute, Tokyo 104-0045, Japan.
[4]Division of Pediatric Oncology, National Cancer Center Hospital, Tokyo 104-0045, Japan.
[5]Division of Genetics, National Cancer Center Research Institute, Tokyo 104-0045, Japan.

The type I interferon (IFN) is a pleiotropic cytokine that can induce antiproliferation, cancer cell death, antiangiogenesis, and immunomodulation, and has been used for the treatment of a variety of cancers, including chronic myelogenous leukemia, melanoma, and renal cancer (Pfeffer *et al.*, 1998; Belardelli *et al.*, 2002). In terms of sarcoma, Müller and co-workers suggested the efficacy of IFN as adjuvant treatment for a high-grade osteosarcoma (Muller *et al.*, 2005). However, clinical experiences with IFN protein therapy for solid tumors have not been encouraging in most of the cases (Einhorn and Grander, 1996). In the conventional regimen of IFN clinical trials, the recombinant IFN protein is systemically administered through subcutaneous or intramuscular routes. As the protein is rapidly degraded in the blood circulation and only a small portion of subcutaneously injected IFN can reach the target sites (Salmon *et al.*, 1996), the limited therapeutic efficacy of treatments with IFN protein reflects the inability to target the cytokine to the right place at a sufficiently high dose. Alternative delivery strategies are needed to achieve a safe and effective IFN delivery. Several animal studies demonstrated that gene- and cell-based delivery of type I IFNs into tumors suppressed the growth of various cancers, such as breast and prostate cancers (Zhang *et al.*, 1996; Hottiger *et al.*, 1999; Ahmed *et al.*, 2001; Benedict *et al.*, 2004; Studeny *et al.*, 2004; De Palma *et al.*, 2008).

Although type I IFN was long thought to act mainly through the direct suppression of tumor cell proliferation *in vivo*, it has recently been established that IFNs have important roles in regulating the innate and adaptive arms of the immune system: up-regulation of major histocompatibility complex (MHC) class I gene, promotion of the priming and survival of T cells, increase of the cytotoxic activity of natural killer (NK) cells and $CD8^+$ T cells, and activation of dendritic cells (DCs) (Ferrantini *et al.*, 2008; Santini *et al.*, 2009). We also reported that, in addition to the direct cytotoxicity at the injected site, an intratumoral IFN gene transfer elicits a systemic tumor-specific immunity in several animal models (Hatanaka *et al.*, 2004; Ohashi *et al.*, 2005; Hara *et al.*, 2007, 2009).

However, the development of effective cancer immunotherapy is often difficult in the clinical setting, because cancer generates an immunotolerant microenvironment against the host immune system (Rabinovich *et al.*, 2007); an additional therapeutic strategy is required to bring a breakthrough. Hematopoietic stem cell transplantation (HSCT) following a preconditioning is expected to introduce a fresh immune system, in which tolerance to tumor cells is not yet induced, and may present an opportunity to augment the efficacy of IFN immune therapy. Furthermore, it has been reported recently that autologous HSCT can induce antitumor immunity by homeostatic proliferation (HP) of T cells following preconditioning-induced lymphopenia. It is known that T-cell HP is driven by the recognition of self antigens, and that the availability of tumor antigens during HP leads to effective antitumor autoimmunity with specificity and memory. The effect is mediated by a reduction in the activation threshold of low-affinity tumor-specific T cells, leading to their preferential engagement and expansion (Baccala *et al.*, 2005; Wrzesinski and Restifo, 2005). Induction of lymphopenia can also enhance cytokine production or increase homeostatic cytokine levels [interleukin (IL)-7, IL-15] by removing cells that compete for these endogenous cytokines (Gattinoni *et al.*, 2005; Wang *et al.*, 2005). In fact, several animal studies showed that lymphopenic conditions alone are able to create an environment sufficient to mount an efficient antitumor immunity (Borrello *et al.*, 2000; Dummer *et al.*, 2002). In this study, we investigated whether a combination of syngeneic HSCT and intratumoral IFN gene transfer induces an effective antitumor immune response against sarcoma.

Materials and Methods

Tumor cell lines and plasmids

143B, U2OS, HOS, MG-63, and HuO 9N2 are human osteosarcoma cell lines. NHOS and LM8 are murine osteosarcoma cell lines, which were derived from BALB/c or C3H mice, respectively. SK-LMS-1, SK-UT-1B, and SKN are human leiomyosarcoma cell lines. SYO1 is a human synovial sarcoma cell line, HT-1080 is a human fibrosarcoma cell line, and RD is a human rhabdomyosarcoma cell line. 143B, U2OS, HOS, and SYO1 cells were maintained in Dulbecco's modified Eagle's medium containing 10% fetal bovine serum (FBS; ICN Biomedicals, Inc., Irvine, CA). HuO 9N2 and NHOS were maintained in RPMI-1640 containing 10% FBS. MG-63, SK-LMS-1, SK-UT-1B, HT-1080, and RD were maintained in Eagle's minimal essential medium containing 10% FBS. SKN was maintained in Ham's F12 medium with 10% FBS. An LM8 cell line that stably expresses the firefly luciferase gene was generated by retrovirus vector-mediated transduction and designated as LM8-Luc.

Plasmids expressing the IFN-α or IFN-β gene under the control of the Rous sarcoma virus promoter were also used for intratumoral gene transfer. The human IFN-α- or IFN-β-expressing plasmids were designated as phIFN-α or phIFN-β, respectively. The mouse IFN-α- or IFN-β-expressing plasmids were designated as pmIFN-α or pmIFN-β, respectively. The plasmids that express an enhanced green fluorescent protein (pEGFP) and luciferase (pLuc) were used as a negative control.

In vitro *IFN gene transfer and cell-proliferation assay*

Culture cells were seeded at $3–8 \times 10^3$ cells/well in 96-well plates 1 day before transfection, and 0.12 μg of plasmid DNA-liposome (Lipofectamine 2000; Invitrogen, Carlsbad, CA) complex was added into each well in accordance with the manufacturer's protocol. The cell numbers were assessed by a colorimetric cell viability assay using a water-soluble tetrazolium salt (Tetracolor One; Seikagaku Corp., Tokyo, Japan). The absorbance was determined by spectrophotometer using a wavelength of 450 nm with 600 nm as a reference. The growth suppression was expressed as the relative cell growth, which was calculated as OD_{450} of pIFN-α- or pIFN-β-transfected cells/OD_{450} of pEGFP-transfected cells. The assays (carried out in six wells) were repeated three times.

Annexin V assay

Cells were seeded at $5–10 \times 10^4$ cells/well in six-well plates 1 day before transfection. A 2-μg plasmid DNA-liposome complex was added to each well. Three days later, the cells were collected and stained with Annexin V-FITC (Medical & Biological Laboratories Co., Ltd., Nagoya, Japan), which detects phosphatidylserine of inverted plasma membranes.

The cells were examined by fluorescence-activated cell sorting (FACSCalibur; BD Biosciences, San Jose, CA). The apoptotic cell death was expressed as specific cell death, which was calculated as the cell death fraction induced by phIFN or pmIFN (%) minus that by pLuc (%). The measurement of the wells was carried out in triplicate, and the means±SD was plotted. The assay was repeated two times.

Cell-cycle analysis

Cells were seeded at $5–10\times10^4$ cells/well in six-well plates 1 day before transfection. A 2-μg plasmid DNA-liposome complex was added to each well, and 3 days later the cells were stained with propidium iodide (PI; Sigma, St. Louis, MO), followed by cell-cycle analysis with flow cytometry. The percentage of the subG$_1$ fraction, which indicates the cell-death population, was calculated compared with the total of the subG$_1$, G$_0$/G$_1$, S, and G$_2$/M phases. A fraction of subG$_1$ shows a major population of cell cycles in some cell lines, which obscures the effect of type I IFN on cell-cycle arrest. Therefore, the percentages of the G$_0$/G$_1$, S, and G$_2$/M fractions were calculated compared with the total of the G$_0$/G$_1$, S, and G$_2$/M fractions except for the subG$_1$ fraction. Then, to demonstrate how the cell cycle is affected by type I IFN expression but not plasmid DNA transfection *per se*, we subtracted the percentages of each cell-cycle phase in pLuc-transfected cells from those in phIFN-α- or phIFN-β-transfected cells, and expressed them as the relative fraction of cells in the cell-cycle phases. The assays were carried out in triplicate.

Animals and IFN-β gene transfer

The sarcoma cells ($5–10\times10^6$) were injected subcutaneously on the legs of BALB/c nude mice (Charles River Japan, Kanagawa, Japan). When the subcutaneous tumor was established (~0.7 cm in diameter), 150 μl of plasmid DNA-liposome complexes was injected directly into the tumors three times every other day. The plasmid DNA-liposome complex was prepared by the addition of 30 μg of plasmid DNA into a total of 75 μl of PBS per mouse, followed by the addition of 75 μl of 0.15 mmol/L DMRIE-DOPE [(±)-*N*-(2-hydroxyethyl)-*N*, *N*-dimethyl-2,3-bis(tetradecyloxy)-1-propanaminium bromide/dioleoylphosphatidylethanolamine] (Vical, Inc., San Diego, CA). The shortest (r) and longest (l) tumor diameters were measured at the indicated days, and the tumor volume was determined as $r^2\times l/2$. Tumor sizes (means±SD) were measured on the days indicated.

For NK cell-depletion experiments, we started the intraperitoneal injection (50 μl) of anti-asialo GM$_1$ antibody (30 mg/ml; Wako Chemicals USA Inc., Richmond, VA) 2 days before the plasmid/liposome administration; the treatment was repeated every 6 days. Animal studies were carried out according to the Guideline for Animal Experiments of the National Cancer Center Research Institute and approved by the Institutional Committee for Ethics in Animal Experimentation.

Hematopoietic stem cell transplantation

Seven- to 9-week-old female BALB/c or C3H mice were purchased from Charles River Japan. The mice received a lethal (9 Gy) irradiation on the day of transplantation, and the irradiated mice were injected intravenously with 5×10^6 bone marrow (BM) cells and 2×10^6 splenic T cells from syngeneic donor mice. BM cells were isolated from donors by flushing each femur and tibia with an RPMI-1640 medium supplemented with 5% FBS (complete RPMI), and splenic cells were prepared by macerating the spleens. After lysis of the erythrocytes, the splenic cells were incubated with anti-Thy-1.2 immunomagnetic beads (Miltenyi Biotec GmbH, Bergisch Gladbach, Germany) at 4°C for 15 min, followed by selection of T cells by AutoMACS (Miltenyi Biotec). Simultaneously, NHOS (3×10^6) or LM8-Luc (5×10^5) cells were injected subcutaneously into the legs of BALB/c or C3H mice, respectively.

ELISpot assay

An IFN-γ ELISpot kit (BD Bioscience) was used according to the manufacturer's instructions. In brief, splenocytes (1×10^5 cells/well) and mitomycin C (MMC)-treated tumor cells (1×10^4 cells/well) were cocultured in 96-well plates precoated with mouse IFN-γ (BD Bioscience) for 20 hr at 37°C in complete RPMI medium in triplicate. MMC was used to prevent proliferation of tumor cells in the culture with lymphocytes. After the wells were washed, a biotinylated anti-mouse IFN-γ antibody (2 μg/ml) was added and incubation continued for 2 hr at room temperature. Then a streptavidin–horseradish peroxidase solution was added and incubation continued for 1 hr at room temperature. After the addition of an aminoethylcarbazole substrate solution, spots were counted under a stereomicroscope.

Cytotoxic assays

The splenocytes were cultured for 4 days with MMC-treated NHOS stimulators, and then the responder cells were collected and used as effector cells. NHOS target cells were labeled with ^{51}Cr (PerkinElmer Japan Co., Kanagawa, Japan). For a 4-hr chromium release assay, 2×10^5, 1×10^5, 5×10^4, and 2.5×10^4 effector cells were mixed with 0.5×10^4 target cells per well in a 96-well round-bottom plate (Corning Inc., Corning, NY). Supernatants were harvested and counted in a gamma counter (Packard Bioscience Company, Meriden, CT). The percentage of cytotoxicity was calculated as [(experimental cpm − spontaneous cpm)/(maximum cpm − spontaneous cpm)]×100. Each assay was done in triplicate.

In vivo *imaging of tumor metastasis*

The C3H mice with LM8-Luc tumors were administered D-luciferin (150 mg/kg) (Wako Pure Chemical Industries) by intraperitoneal injection. Ten minutes later, photons from animal whole bodies were counted using an *in vivo* imaging system (IVIS; Xenogen, Alameda, CA).

Immunohistochemistry and TUNEL assay

Immunostaining was performed using the streptavidin–biotin–peroxidase complex techniques (Nichirei, Tokyo, Japan). Consecutive cryostat tissue sections (6 μm) were mounted on glass slides and fixed in 99.5% ethanol for 20 min. After blocking with normal rat serum, the sections were stained with rat anti-mouse CD4 and CD8 antibodies (BD Biosciences). The cryostat sections were also processed for the terminal deoxynucleotidyltransferase-mediated

dUTP-digoxigenin nick-end-labeling (TUNEL) assay (ApopTag *in situ* apoptosis detection kit; Intergen Company, Purchase, NY). Negative controls without primary antibodies were examined in all cases. The sections were counterstained with methyl green.

Statistical analysis

Two-sided *t* tests were used to validate the significance of the observed differences, which were considered statistically significant when $p < 0.05$.

Results

Transfection of IFN plasmid suppressed cell growth

First, to examine the gene-transduction efficiency, a variety of sarcoma cell lines, one lung cancer cell line, and one prostate cancer cell line were transfected with pEGFP in six-well plates. Flow cytometry showed that the percentage of $EGFP^+$ cells varied [1.6% (LM8) to 75.9% (HT1080)]; however, it was less than 20% in almost all cell lines except for two cell lines (Fig. 1A). Next, to compare the expression levels of IFN-α and IFN-β with the gene-transduction efficiency the IFN concentration was measured in the supernatants of IFN plasmid-transfected cells. The enzyme-linked immunosorbent assay (ELISA) showed that the IFN concentrations were also different; however, they appeared to be related to the gene-transduction efficiency (Fig. 1B). The IFN-α concentration was generally higher than the IFN-β concentration in each cell line (Fig. 1B). The IFN-α gene might be more effectively translated than the IFN-β, or the IFN-α protein might be more stable than IFN-β in the supernatant of the culture cells.

To examine whether the expression of IFN gene effectively inhibits the growth of osteosarcoma cells, four human osteosarcoma cell lines and one mouse osteosarcoma cell line (NHOS) were transfected with pIFN-α or pIFN-β. The transfection of the IFN plasmid inhibited the growth of all osteosarcoma cells to less than 40% of that of the control plasmid (pEGFP)-transfected cells, whereas the growth suppression was less conspicuous in the prostate (PC3) and lung (A549) cancer cells (Fig. 1C). Then, to investigate the growth-suppressive effect of IFN gene transduction in various human soft-tissue sarcoma cell lines, phIFN-α or phIFN-β was introduced to one rhabdomyosarcoma, one fibrosarcoma, one synovial sarcoma, and two leiomyosarcoma cell lines. IFN expression significantly suppressed cell growth in all sarcoma cell lines (Fig. 1D).

To examine cell-death induction by IFN gene transduction, Annexin V assay was performed in various sarcoma cell lines transfected with the IFN-α or IFN-β plasmid. The assay showed that IFN expression effectively induced apoptosis in many osteosarcoma cell lines and soft-tissue sarcoma cell lines. IFN-β gene transfer was more effective in inducing cell death than IFN-α gene transfer in most sarcoma cell lines (Fig. 1E and F). Although the suppression of cell growth and induction of apoptosis were more effective in the sarcoma cells as compared with the prostate and lung cancer cells, it was not closely related to the IFN concentration; for example, the transfected A549 cells produced a relatively high IFN level, but the apoptosis induction was less conspicuous, suggesting that sarcoma cell lines are susceptible to type I IFN expression. The IFN concentration may not be increased in the IFN-sensitive cells due to the decrease of cell number by apoptosis induction.

Furthermore, to examine the effect of IFN gene transduction in the cell cycle, three sarcoma cell lines and one lung cancer cell line were transfected with phIFN-α or phIFN-β. Flow cytometry showed that the $subG_1$ fraction was significantly increased in the IFN-β-transduced cells compared with the IFN-α-transduced cells (Fig. 1G), which confirmed the results of the Annexin V assay. In terms of the effect of IFN on the cell cycle, it has been reported that type I IFN induces G_1 cell-cycle arrest in renal cancer cells (Shang *et al.*, 2011) and G_2/M arrest in hepatocellular carcinoma (Fujioka *et al.*, 2006) and colon cancer cells (Barnes *et al.*, 2003). In this study, IFN-α transduction increased the percentage of cells in a G_2/M phase in sarcoma cell lines (Fig. 1G). The cell growth inhibition by IFN-α transduction was similar to IFN-β in the cell-proliferation assay (Fig. 1C and D). Although the cell-death induction was effectively induced by IFN-β, IFN-α also was able to significantly induce apoptosis, and the G_2/M arrest by IFN-α transduction might add to the apoptosis induction.

Antitumor effect of intratumoral IFN-β gene transfer in subcutaneous tumor model

To examine the antitumor effect of IFN-β gene transfer *in vivo*, 143B human osteosarcoma or SK-UT-1B human leiomyosarcoma cells were inoculated on the legs of BALB/c nude mice, and then a phIFN-β-liposome complex was injected directly into the tumors three or six times. The growth of the 143B tumor was more rapid than that of the SK-UT-1B tumor. The IFN-β gene transfer showed a significant suppressive effect against the 143B tumors in a dose-dependent manner, whereas a three-time injection of phIFN-β-liposome was sufficient to eradicate the SK-UT-1B tumors (Fig. 2A). The ELISA showed that the IFN-β expression in the 143B subcutaneous tumors continued for more than 7 days after intratumoral injection of phIFN-β (30 μg) three times (Fig. 2B).

Then, to examine whether the human IFN-β expression induces cell death in the tumors, the TUNEL assay was performed using tumors of mice treated with human IFN-β gene transfer. The assay revealed the cell death of many cancer cells in the phIFN-β-transfected 143B tumors (Fig. 2C).

As mouse IFN shows no cross-species activity in human cells, it does not directly induce cell death in 143B or SK-UT-1B tumors, whereas mouse, but not human, type I IFN can enhance the cytotoxicity of mouse immune cells, such as NK cells (Ohashi *et al.*, 2005). To examine whether mouse IFN-β gene therapy leads to suppression of human osteosarcoma xenografts in nude mice, 143B or SK-UT-1B cells were inoculated on bilateral legs of BALB/c nude mice, and a pmIFN-β-liposome complex was injected directly into the tumors three times. The mouse IFN-β gene transfer significantly suppressed growth of not only the transfected right tumors, but also of the untransfected left tumors (Fig. 2D). The results indicated that an intratumoral IFN-β gene transfer effectively induces systemic antitumor immunity. To confirm that mouse IFN-β gene transfer activated the NK cells, the mice were treated with an anti-asialo GM1